전 용 필 교수 지도

석사학위 청구논문

Anti-Müllerian Hormone (AMH) Intermediates Ovarian Reservation and Ovarian Aging

2020

성신여자대학교 일반대학원

생물학과

김주혜

전 용 필 교수 지도

석사학위 청구논문

Anti-Müllerian Hormone (AMH) Intermediates Ovarian Reservation and Ovarian Aging

2020

성신여자대학교 일반대학원

생물학과

김주혜

Anti-Müllerian Hormone (AMH) Intermediates Ovarian Reservation and Ovarian Aging

Adviser: Yong-Pil Cheon, Ph.D.

A thesis submitted in partial
fulfillment of the requirements for the
Degree of Master of Science

November, 2019

Department of Biology

Graduate School

Sungshin University

Kim, Juhye

Certificate of Committee Approval

Be accepted partial fulfillment of the requirements for the degree of:
Master of Science

Signatures:

Chairperson	Park, Jong Hyuk, Ph.D
Committee member	Chun, Min-Young, MD
Committee member	Cheon, Yong-Pil, Ph.D

Sungshin University

Graduate School

ABSTRACT

Anti-Müllerian hormone (AMH) Intermediates Ovarian Reservation and Ovarian Aging

Kim, Juhye
Department of Biology
Graduate School
Sungshin Women's University

In female, anti-Müllerian hormone (AMH) is released from granulosa cells of growing follicles and inhibits primordial-primary follicle transition and reduces FSH-sensitivity to develop preantral follicles to antral follicles. Therefore, AMH is considered to be related to ovarian aging. Indeed, AMH serum level decreases by aging. Old (7 - 11 months) female *Amh* knockout (KO) mice tended to have lower delivery rate, compared to wild type animals in the same range of age. The ovarian weight was increased until 7 month in wild type mice but decreased at 7 month in *Amh* KO mice. Relative ovaian weight to body weight was no changed after maturation but not in *Amh* KO mice. We conducted qPCR on ovaries targeting *Kitl*, *Kit*, *Gdnf* and *Gfra1* which are known to involve in primordial-primary follicle transition. The numbers of primordial follicles were significantly many in *Amh* KO mice in ≥ 6 wk and ≥ 3 m

groups than wild type mice in same age groups. However, its number was significantly fewer in *Amh* knockout mice than wild type mice of the same age groups. *Kitl*, *Kit*, *Gdnf*, *Gfra1* and *Bmpr1a* mRNAs gradually increased by aging after maturation. However, expression profiles in *Amh* KO mice were different from wild type. The expression levels of *Bmpr1a* mRNA, type I receptor of AMH, decreased in ≥ 3 m and ≥7 m *Amh* KO groups, compared to wild type. On the other hand, ratio of p-YAP/YAP was significantly decreased from 6 wks to older age. Based on these results, it is suggested that AMH may control primordial-primary follicle transition and ovarian reservation by YAP signaling.

CONTENTS

List of Tables

List of Figures

INTRODUCTION

Anti-Müllerian hormone (AMH), also known as Müllerian-inhibiting substance (MIS), is a member of the transforming growth factor-β (TGFβ) superfamily of peptide growth and differentiation factors. It is well known gene for sex differentiation during fetal development. In female, AMH is expressed in granulosa cells (GCs) of growing follicles and detected from neonatal stages. Especially it is abundant from secondary to small antral follicle stages, whereas only weak signal is detected in primary follicles (Hirobe *et al.*, 1992). *Amh* mRNA starts being detected in ovarian granulosa cells from postnatal day 3 onward in Sprague Dawley rats (Hirobe *et al.*, 1992). *Amh* expression disappears when follicles become 500 μm preovulatory or atretic (Hirobe *et al.*, 1992). There is no marked change in *Amh* and *AmhrII* mRNA expression during estrous cycle, while heterogeneous decrease in mRNA expression of both at estrus is found in nonatretic preantral follicles (Baarends *et al.*, 1995).

The target organ for AMH in male fetus is Müllerian duct as its name. *Amh* null male mammals develop Müllerian duct derivatives such as oviducts, a uterus, and a vagina, besides a complete male reproductive system (Behringer *et al.*, 1994). The *Amh*-deficient males can produce functional sperm, but most of them are sterile, as female organs block sperm transfer into females (Behringer *et al.*, 1994). The *Amh* null mouse is an excellent model for examining the function of AMH in the mouse ovary, as AMH and AMHRII are

predominantly found in the postnatal ovary in female animals, so nonovarian effects of the deletion of the *Amh* gene are unlikely to occur (Durlinger *et al.*, 1999). AMH null female mammals have macroscopically normal uteri, oviducts, and ovaries. The females are fertile and have normal litter size (Durlinger *et al.*, 1999).

As a member of the TGFβ super family, it is thought that AMH uses the signal transduction system that has been identified for the other family members like TGFβ, activin and the bone morphogenetic proteins (BMPs) (Zec *et al.*, 2011). These factors signal through a serine-threonine kinase receptor complex which consists of ligand-specific type II receptors and more general type I receptors, also known as activin receptor-like protein kinases (ALKs). An activated receptor complex phosphorylates and activates cytoplasmic SMAD proteins, which translocate to the nucleus and directly or indirectly regulate gene expression. Type II receptor of AMH is AMHRII.

AMH inhibits primordial-primary follicle transition and reduces FSH-sensitivity to develop preantral follicles to antral follicles (Zec *et al.*, 2011). Because of the function, it is considered to be related to ovarian aging which is defined as decline of the ovarian reserve with age. Ovarian reserve indicates quantity and quality of primordial follicle pool. Indeed, by aging AMH serum levels decreased in many studies (de Vet *et al.*, 2002). In a study aged 13-month-old *Amh* KO mice had largely decreased primordial follicle pool compared to wild type, demonstrating that deletion of AMH accelerates primordial follicle depletion (Durlinger *et al.*, 1999).

Glial cell-line-derived neurotrophic factor (GDNF) and kit ligand (KITL) promotes primordial follicle development and work through each of their receptor GDNF receptor α1 (GFR α1) and KIT proto-oncogene receptor tyrosine kinase (KIT) (Dole G *et al.*, 2008).

The core cascade of Hippo pathway in mammals is consisted of Sterile 20-like kinase I/II (MST1/2), large tumor suppressor 1/2 (LATS1/2), transcriptional coactivator, Yes-associated protein (YAP) and another transcriptional effector, transcriptional co-activator with PDZ-binding motif (TAZ) (Meng Z *et al.*, 2016). When YAP and TAZ are activated they translocate into nuclei and induce transcription of genes that are related to cell proliferation, differentiation, migration. YAP/TAZ is inactivated by phosphorylation. It was suggested that primordial follicle activation is related to decrease in ratio of phosphorylated YAP1 (p-YAP)/YAP1 (Xiang C *et al.*, 2015). Ovarian fragmentation decreased p-YAP and increased nuclear localization of YAP, leading to follicle growth (Kawamura *et al.*, 2013).

In this study, it was studied whether inhibition of *Amh* induces early ovarian failure, eventually, lower delivery rate. We demonstrated tendency of mRNA level changes of *Kitl*, its receptor, *Kit*, Gdnf and *Gfrα1* which involve in primordial -primary follicle transition by aging and whether AMH regulates follicle recruitment by inhibiting those genes. We also showed mRNA level changes of *Bmpr1a*, an AMH type I receptor. Furthermore, YAP/p-YAP protein levels were analyzed.

MATERIALS AND METHODS

Experimental animals

All animal procedures were approved by the institutional Animal Care and Use Committee (IACUC) of Sungshin University (SSWIACUC-2019-005). Male and female wild type, heterozygous and homozygous B6;129S7-*Amh*^{tm1Bhr}/J mice (Jackson Laboratory) were conducted in accordance with the Guide for the Care and Use of Laboratory Animals published by the National Institute of Health and maintained under standard condition at the animal house of Sungshin University. Circadian rhythm was kept under the 14L:10D schedule with light-on at 06:00 and clean room system. Animals were fed a standard rodent diet and water ad libitum from. To genotype the mice, ear tissues were collected and gDNA was extracted from the tissues. Conventional PCR was conducted with the gDNA and electrophoresis was performed with the PCR products on 1.5% agarose gel, then UV was projected on the gel to detect DNA bands (Table 1, Fig. 1). Wild type produced 243 bp, *Amh* KO produced 280 bp and heterozygote produced both 243 and 280 bp bands. Information of the primers which were used for genotyping is available on Table 3. Maximum 3 sexually mature females (over 6 weeks) per male (over 10 weeks) were bred for 2 weeks. The groups were divided by age, such as postnatal day (PND) 3 wk, PND 42 - 89 (≥ 6 wk), PND 90 - 149 (≥ 3 m), PND 210 - 329 (≥ 7 m).

Ovarian follicle count

The overnight-fixed ovaries were dehydrated in alcohol series using Leica TP 1020, and embedded in paraffin using Leica EG 1150 H. The paraffin block was serial-sectioned at 4 μm using Leica RM2245 microtome and 75th, 95th and 115th or their neighbor sections were stained with hematoxylin and eosin Y. Tissues were microphotographed using Olympus BX60 microscope and Olympus DP71 microscope digital camera. Adopting the following classification, follicular stages were defined as (1) primordial follicles: follicles with one layer of flattened granulosa cells surrounding an oocyte, (2) primary follicles: follicles with one layer of cuboidal granulosa cells, (3) secondary follicles: follicles with two or more layers of cuboidal granulosa cells, (4) tertiary follicles: follicles where a cavity in the granulosa cells appear and/or antrum formation begins, (5) preovulatory follicles: follicles with large antrum (Fig. 3A). To count more representative number of follicles in an ovary in confined few sections, primordial and primary follicle counts on the each three sections were summed, and the largest numbers of secondary, tertiary and preovulatory follicle and corpus lutea among the three sections were chosen, considering follicle sizes and the thickness of a section.

Total RNA extraction

Total RNA was extracted using TRI reagent (Cat #: TR 118,

Molecular Research Center, Cincinnati, OH, USA) according to manufacturer's instruction with modification. Briefly, the sample was homogenized with TRI reagent (1 mL/100 mg) and kept for 10 min at room temperature (RT). The chloroform (200 μL/mL) was added and shaken vigorously for 15 sec. Then the mixture was stored for 15 min at RT and centrifuged at 12,000 g for 15 min at 4℃. The RNA was precipitated by mixing isopropanol (0.5 mL/mL), inverting several times, maintaining at RT for 10 min, and centrifuging at 12,000 g for 8 min at 4℃. Purity and concentration of total RNA were assessed by NanoDrop 2000 Spectrophotometer (Cat #: ND-2000, Thermo Scientific, Wilmington, DE, USA). The total RNA was stored at -80℃ until used.

First strand cDNA synthesis

First strand cDNA was synthesized using AccuScript High Fidelity Reverse Transcriptase (Cat #: 600089, Agilent Technologies, CA, USA) according to the manufacturer's instruction. Shortly, reaction reagents were total RNA, AccuScript 10× RT buffer 5.0 μL, 0.5 μg/μL oligo dT primer 1.0 μL, 0.1 μg/μL random primers 1.0 μL, 100 mM dNTP mix 2μL, and RNase-free DEPC-treated water. Reaction mixture was incubated at 65℃ for 5 min, and cooled slowly at RT to allow the primers to anneal to RNA for 10 min. Next, 100 mM DTT 4.0 μL, 40 U/μL RNase block ribonuclease inhibitor 2.0 μL (Cat #: 30015251, Agilent Technologies, CA, USA), and AccuScript High Fidelity RT 1.0 μL were added. The mixture was incubated for at 42℃ for 1

hr and at 70℃ for 10 min to terminate cDNA synthesis. cDNA was stored at -20℃.

Real-Time PCR

Real-time PCR was performed on the mix of reagents as followings, 40 ng/㎕ cDNA 1 ㎕, each sense and anti-sense 1 ㎕, distilled water 7 ㎕ and TB green Premix Ex TaqTM (Cat #: RR420A, TaKaRa, Japan) 10 ㎕ in Thermal Cycler Dice Real Time System TP800 (TaKaRa, Japan). Each reaction was run in triplicate. Dissociation curves were run on all reactions to ensure amplification of a single product with the appropriate melting temperature (Table 2). The primer information is available on Table 3. The fold change in gene expression was calculated using the ⊿⊿Ct method with housekeeping gene, 36B4, as an internal control.

Protein extraction and Western blotting analysis

Ovaries were homogenized in cold homogenization buffer (50 mM Tris-Cl, 150 mM NaCl, 10 mM β-mercaptoethanol, 2 mM $CaCl_2$, 0.1 mM PMSF, 1 ㎛M Leupeptin, 1 ㎛M Pepstatin, 0.5 mM EDTA, 15% Glycerol, 0.1% NP-40). The homogenates were centrifuged to remove insoluble materials. The protein concentration was determined using protein dye reagent (Cat #: #500-0205, Bio-Rad Laboratories, Inc., CA, USA) by Bradford assay. 30 ㎍/ml of protein were boiled in SDS/β-mercaptoethanol sample buffer, and loaded onto each lane of 10% SDS-PAGE. The proteins were separated by

electrophoresis and then electrotransferred onto polyvinylylidene difluoride (PVDF) membranes (Cat #: 10600023, General Electric Healthcare, USA) in transfer buffer (25 mM Tris base, 192 mM Glycine, 0.1% SDS, 20% Methanol, pH 8.3). The membranes were blocked in 5% skimmed dry milk in TBST buffer (10 mM Tris-HCl, 150 mM NaCl, 0.05% Tween-20) for 1 hr at RT, and washed three times with TBST. The membranes were incubated overnight at RT with rabbit monoclonal YAP/TAZ antibody (dilution 1:1000) and mouse monoclonal GAPDH antibody (dilution 1:4000) or for 30 min with rabbit polyclonal YAP (phospho-Ser127) antibody (dilution 1:1000) and mouse monoclonal GAPDH antibody (dilution 1:4000). After incubation, membranes were washed three times and incubated for 30 min with horseradish peroxidase conjugated goat anti-rabbit IgG (dilution 1:5000) or horseradish peroxidase conjugated goat anti-mouse IgG (dilution 1:5000). The bands were developed with Amersham ECL Prime Western Blotting Detection Reagent (Cat #: RPN2232, General Electric Healthcare, USA) and detected by ChemiDoc MP Imaging System (Cat #: 17001402, Bio-Rad Laboratories, Inc., CA, USA). The intensity of each band was normalized with total protein using Imagej software. Information of the antibodies is presented in Table 4.

Statistics

The Student's t-test was performed to evaluate the statistical significance between control and experimental

group. Results were presented as mean ± SD. Significance of fertility data was evaluated by chi-square test. Statistical significance was considered at $p<0.05$.

Table 1. Conventional PCR thermal cycler schedule for genotyping

step		Temperature (℃)	Time
Hold	Hold	94	3 min
3 step PCR (11 cycle)	Denaturation	94	30 sec
	Annealing	64	30 sec
	Extension	72	35 sec
3 step PCR (24 cycle)	Denaturation	94	20 sec
	Annealing	58	30 sec
	Extension	72	35 sec
Hold	Hold	72	2 min
		10	Indefinitely

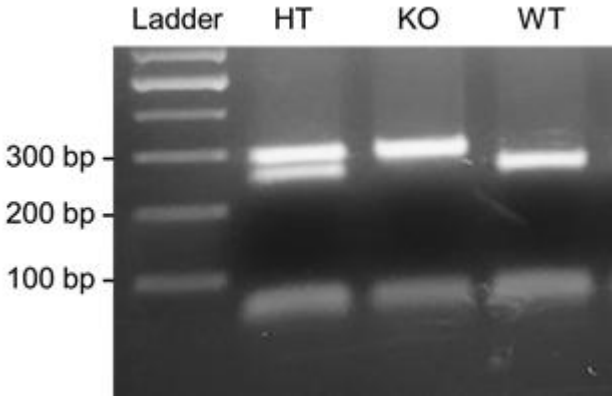

Fig. 1. Genotyping of the *Amh* KO mice line. The first lane is 100 bp step DNA ladder (Cat #: BNL005, Bionics). The second is DNA bands of a heterozygous *Amh* KO mouse, presenting bands of both wild type and KO mice. The third is a band of an *Amh* KO mouse. The fourth is a band of a wild type mouse. The DNA band size of wild type is 243 bp and *Amh* KO, 280 bp.

Table 2. qPCR thermal cycler schedule

step		Temperature (℃)	Time
Hold	Hold	95	30 sec
3 step PCR (45 cycle)	Denaturation	95	1 min
	Annealing	59	30 sec
	Extension	72	1 min
Dissociation	Denaturation	95	15 sec
	Annealing	60	30 sec
	Extension	95	15 sec
Hold		4	Indefinitely

Table 3. Primer information

Gene	Symbol	NCBI gene reference		Primer sequence (5'-3')
anti-Müllerian hormone	*Amh* WT	NM_007445.3	S	GGAACACAAGCAGAGCTTCC
			AS	GAGACAGAGTCCATCACGTACC
	Amh KO		S	CTTGGGTGGAGAGGCTATTC
			AS	AGGTGAGATGACAGGAGATC
kit ligand	*Kitl*	NM_013598.3	S	GCGGGAATCCTGTGACTGATAATG
			AS	CATGCATAACACGAGGTCATCCA
KIT proto-oncogene receptor tyrosine kinase	*Kit*	NM_001122733.1	S	CGGAGCCCACAATAGATTGGTA
			AS	AACTCTTGCCCACATCGTTGG
glial cell line derived neurotrophic factor	*Gdnf*	NM_010275.3	S	ATTGCAGCGGTTCCTGTGAATC
			AS	TCTTCGCACTGTAGCAGGAATG
glial cell line derived neurotrophic factor family receptor alpha 1	*Gfra1*	NM_010279.3	S	CAGAGTCAAGGTCTGTCAGCAACTG
			AS	ACATCCGAGCCATTGCCAAA
bone morphogenetic protein receptor, type 1A	*Bmpr1a*	NM_009758.4	S	TGTAAGGAAGCCTCCCTCATTCAC
			AS	TTCTGGCTTCTTCTGGTCCAAGTC

Table 4. Antibody information for western blot

Name	Catalog Number	Company
YAP/TAZ – Rabbit monoclonal	#8418	Cell Signaling
p-YAP – Rabbit polyclonal	orb99152	Biorbyt
GAPDH – Mouse monoclonal	sc-32233	Santa Cruz

RESULTS

7-month - 11-month-old *Amh* KO mice had tendency to lower delivery rate

wild type female mice ≥ 6 wk had 66.67%, ≥ 3 m had 77.78% and ≥ 7 m had 51.43% delivery rate with wild type male (Fig. 2). Delivery rate decreased in aged female mice ≥ 7 m. *Amh* KO female mice ≥ 6 wk had 53.33%, ≥ 3 m had 90% and ≥ 7 m had 31.82% delivery rate with wild type male. Delivery rate was dropped in old female mice ≥ 7 m like wild type but more sharply, as ≥ 7 m tended to have lower delivery rate, even though it was not significantly different compared to wild type animals in the same range of age (P = 0.146355).

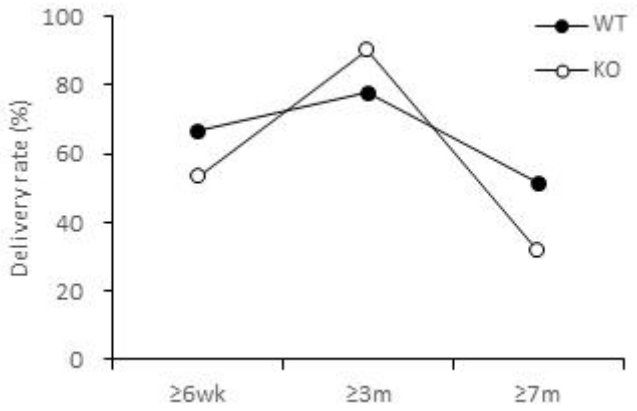

Fig. 2. Female age- and genotype-dependent delivery rate. Closed circle represents wild type and opened circle represents *Amh* KO female mice bred with male for 2 weeks. Statistical significance between genotypes was assessed by chi-square test at $P < 0.05$.

Ovary weights of immature *Amh* KO mice increased and relative ovary weights of *Amh* KO mice decreased compared with immature mice

In wild type groups, body, uterus, ovary and body weight-relative uterus were heavier than those of immature 3 wks old wild type mice. The relative ovary weights to body weight didn't significantly change (Table 5). However, in *Amh* KO mice groups, relative ovary weights to body weight significantly changed with decreasing. When the *Amh* KO mice data were compared with the data of wild type groups in each of the same range of age, 3-week-old *Amh* KO mice had higher both absolute and relative ovary weights and *Amh* KO ≥ 7 m had lower relative ovary weight. *Amh* KO ≥ 3 m didn't show any significant difference because of high standard deviation value.

Table 5. Body, uterus and ovary weight profile.

Group	Body weight (g)	Uterus weight (mg)	Ovary weight (mg)	Uterus/body weight	Ovary/body weight
WT 3 wk	7.22±1.73	3.79±1.23	0.943±0.493	$5.172\times10^{-4}\pm5.530\times10^{-5}$	$1.244\times10^{-4}\pm3.720\times10^{-5}$
WT ≥ 6 wk	17.38±2.03[a]	24.98±16.13[a]	2.617±1.180[a]	$1.365\times10^{-3}\pm7.930\times10^{-4a}$	$1.475\times10^{-4}\pm5.965\times10^{-5}$
WT ≥ 3 m	19.73±1.47[a]	41.92±12.55[a]	2.570±0.533[a]	$2.107\times10^{-3}\pm5.285\times10^{-4a}$	$1.302\times10^{-4}\pm2.478\times10^{-5}$
WT ≥ 7 m	23.66±1.81[a]	64.27±6.72[a]	3.300±0.501[a]	$2.718\times10^{-3}\pm2.249\times10^{-4a}$	$1.398\times10^{-4}\pm2.057\times10^{-5}$
KO 3 wk	7.40±0.52	4.23±0.72	1.450±0.176[c]	$5.692\times10^{-4}\pm6.298\times10^{-5}$	$1.958\times10^{-4}\pm1.835\times10^{-5c}$
KO ≥ 6 wk	17.59±0.81[b]	31.90±0.14[b]	2.675±0.568[b]	$1.816\times10^{-3}\pm9.203\times10^{-5b}$	$1.523\times10^{-4}\pm3.364\times10^{-5b}$
KO ≥ 3 m	19.01±4.83	32.75±37.55	3.575±2.074	$1.521\times10^{-3}\pm1.589\times10^{-3}$	$1.770\times10^{-4}\pm7.339\times10^{-5}$
KO ≥ 7 m	24.63±1.33[b]	75.72±21.50[b]	2.800±0.730[b]	$3.050\times10^{-3}\pm7.205\times10^{-4b}$	$1.138\times10^{-4}\pm2.890\times10^{-5b,c}$

a, $P < 0.05$ compared with WT 3 wk

b, $P < 0.05$ compared with KO 3 wk

c, $P < 0.05$ compared with the wild type in the same range of age

Amh KO mice had fewer follicles

Compared with wild type, the number of primordial follicles in *Amh* KO ovaries was not different in the 3 wk group (Fig. 3, Fig. 4A). Increase in the ≥ 6 wk and ≥ 3 m groups was observed, but it decreased in the ≥ 7 m group. We anticipated that the number of primary follicles would be increased in the young mature *Amh* KO group following accelerated primoridal-primary follicle transition, and then decreased in the old *Amh* KO group by depletion of primordial follicles, the source of primary follicles. Even if it decreased in ≥ 6 wk group, it also decreased in the ≥ 7 m group (Fig. 4B). Secondary follicle counts were similar to the primary follicle counts (Fig. 4C). As preantral-antral follicle transition is induced in *Amh* KO mice, the number of tertiary follicles increased in the ≥ 6 wk group and decreased in the ≥ 7 m group (Fig. 4D). Preovulatory follicle counts didn't show significant difference (Fig. 4E). Corpus lutea (CL) indicate ovulation, and so immature mice didn't have CL (Fig. 4F). However, it was different from our expectation that ≥ 7 m *Amh* KO had significantly more CL.

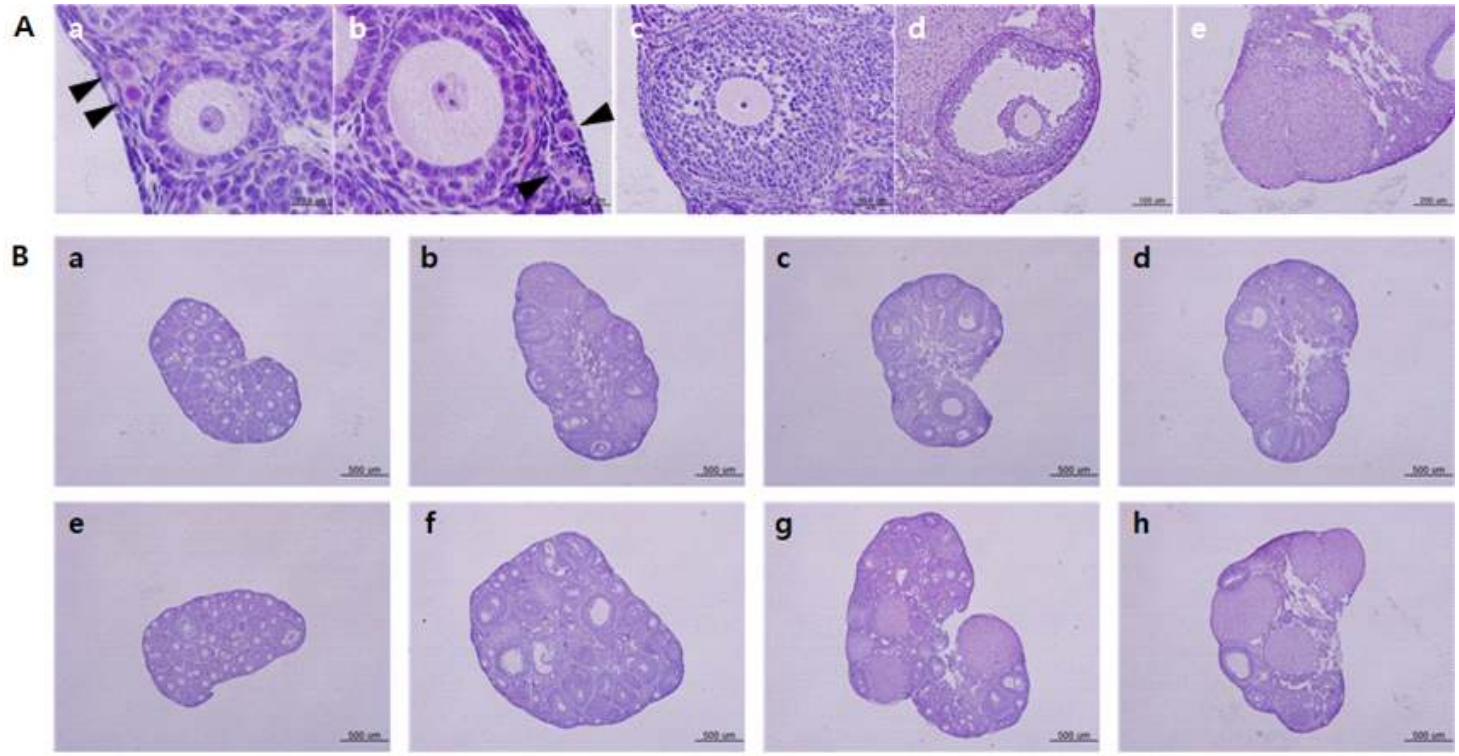

Fig 3. Ovarian follicles. (A) Representative microphotographs of stages of follicles. a, Primordial (arrowhead) and primary follicle. b, Primordial and secondary follicle. c, Tertiary follicle. d, Preovulatory follicle. e, corpus luteum (CL). (B) Representative microphotographs of ovaries of experimental groups. a-d, wild type. e-h, *Amh* KO. a,e, 3-week-old. b,f, ≥ 6-week-old. c,g, ≥ 3-month-old. d,h, ≥ 7-month-old.

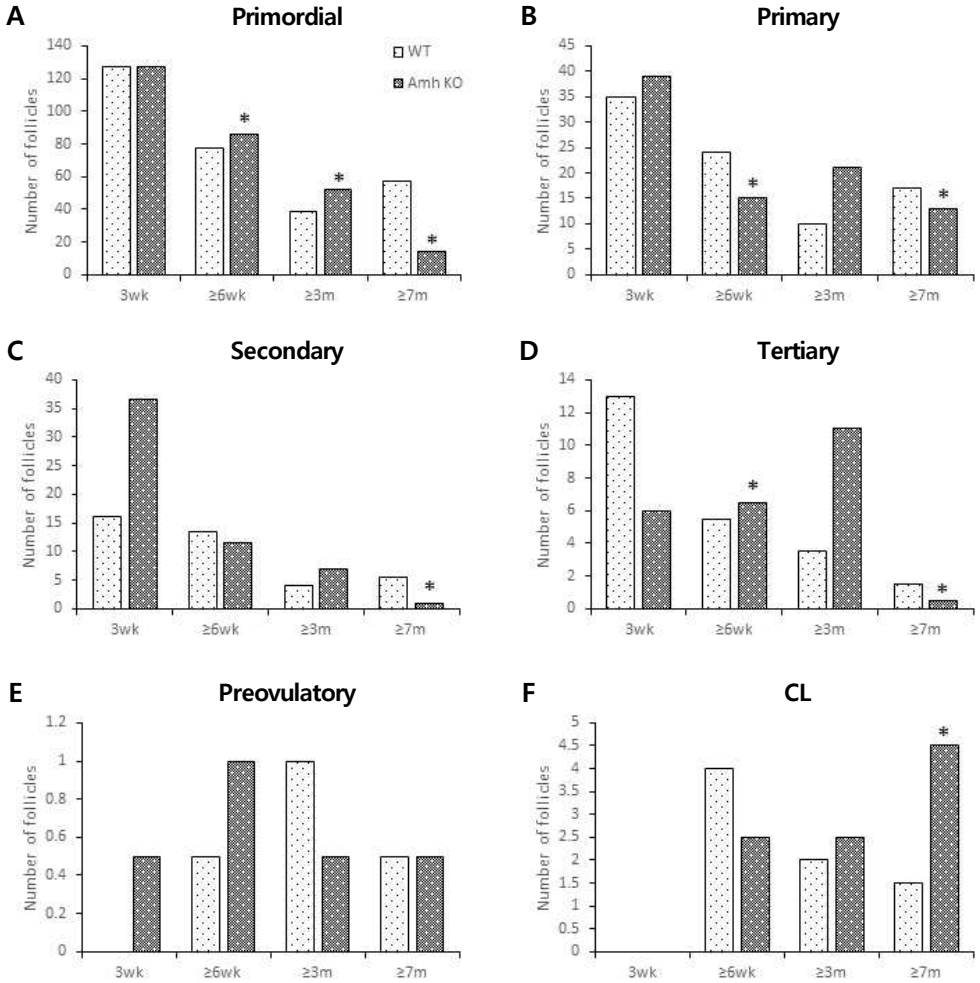

Fig. 4. Numbers of follicles. (A) Primordial, (B) primary, (C) secondary, (D) tertiary and (E) preovulatory follicles and (F) corpus lutea were counted on wild type and *Amh* KO mouse ovaries. Statistical significant difference was evaluated between same age groups of wild type and *Amh* KO mice. $*P < 0.05$.

Kitl increased by aging in wild type and decreased in aged *Amh* KO mice

Kit ligand involves in primordial-primary follicle transition that is also known that AMH has inhibition action on it. If To discover tendency of mRNA level changes by aging and if *Amh* regulates follicle recruitment by inhibiting the genes. In wild type groups compared with immature mice, *Kitl* mRNA level decreased in ≥ 6 wk but increased in older age groups gradually by aging (Fig. 5A). In *Amh* KO groups compared with immature mice, *Kitl* decreased in ≥ 6 wk and ≥ 3 m (Fig. 5B). Compared with the wild type groups in the same range of age, *Kitl* increased in *Amh* KO 3 wk and decreased in *Amh* KO ≥ 3 m and ≥ 7 m (Fig. 5C-F). If *Kitl* was inhibited by *Amh* to block primordial-primary follicle transition, it would be increased by deletion of Amh. However, *Kitl* decreased in the aged *Amh* KO group, so these results suggest that *Amh* doesn't suppress primordial-primary follicle transition by inhibiting *Kitl*.

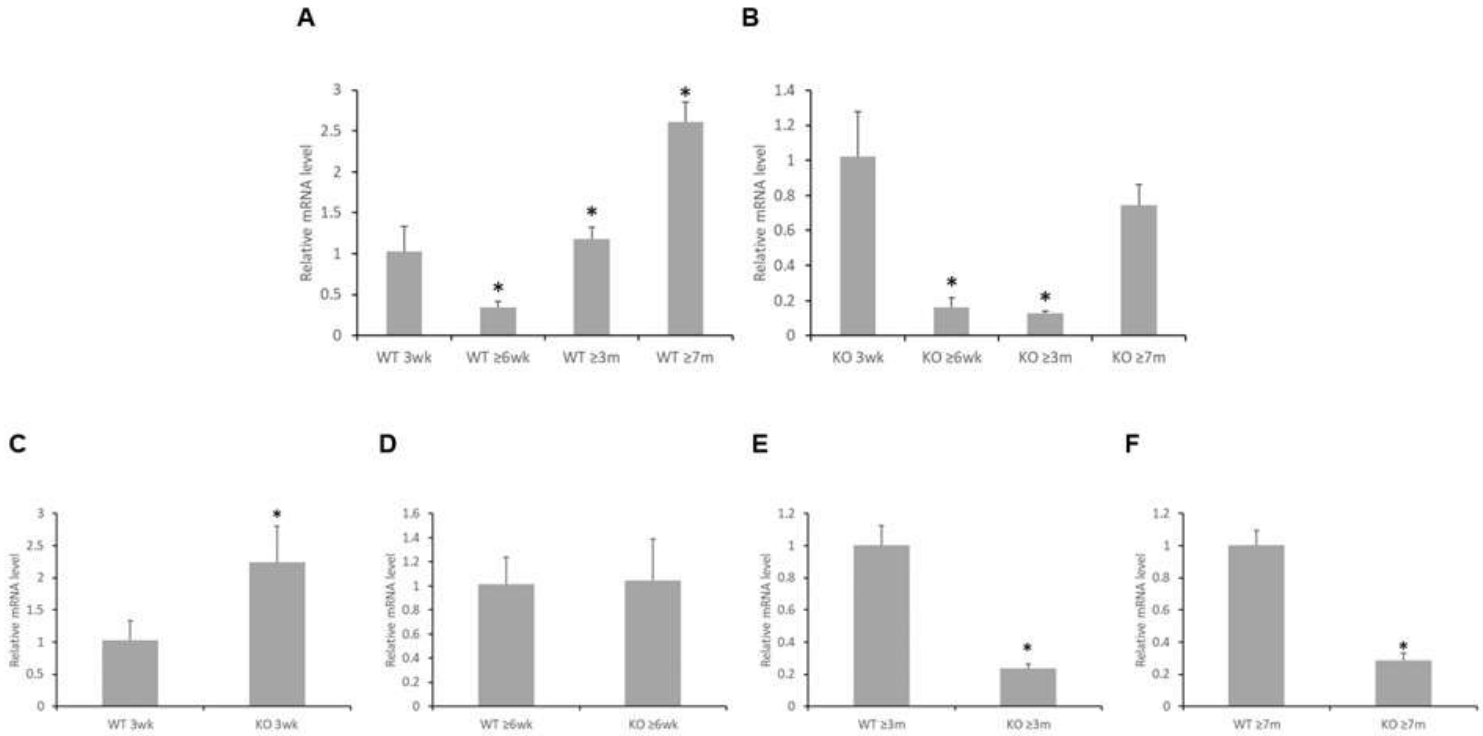

Fig 5. Relative *Kitl* mRNA level on mouse ovaries. (A – B) Relative *Kitl* mRNA level changes in (A) wild type and (B) *Amh* KO mice by aging. Statistical significance was evaluated versus 3-week-old wild type animals. (C – F) Relative *Kitl* mRNA level changes in *Amh* KO (C) 3 wk, (D) ≥ 6 wk, (E) ≥ 3 m and (F) ≥ 7 m mice, compared with wild type mice. Data are presented as means ± standard deviation. $*P < 0.05$.

Kit increased by aging in wild type and decreased in aged *Amh* KO mice

c-kit also involves in primordial-primary follicle transition as the receptor of kit ligand. In wild type mice relative *Kit* mRNA level increased in ≥ 3 m and ≥ 7 m (Fig. 6A). In *Amh* KO mice *Kit* decreased in all of ≥ 6 wk, ≥ 3 m and ≥ 7 m (Fig. 6B). Compared with the wild type groups in the same range of age, *Kit* increased in *Amh* KO 3 wk and decreased in *Amh* KO ≥ 6 wk, ≥ 3 m and ≥ 7 m (Fig. 6C-F). The general expression pattern was similar to its ligand, *Kitl*. Like *Kitl*, *Kit* decreased in aged *Amh* KO mice, so it is suggested that *Amh* doesn't inhibit primordial-primary follicle transition by controlling *Kit* either.

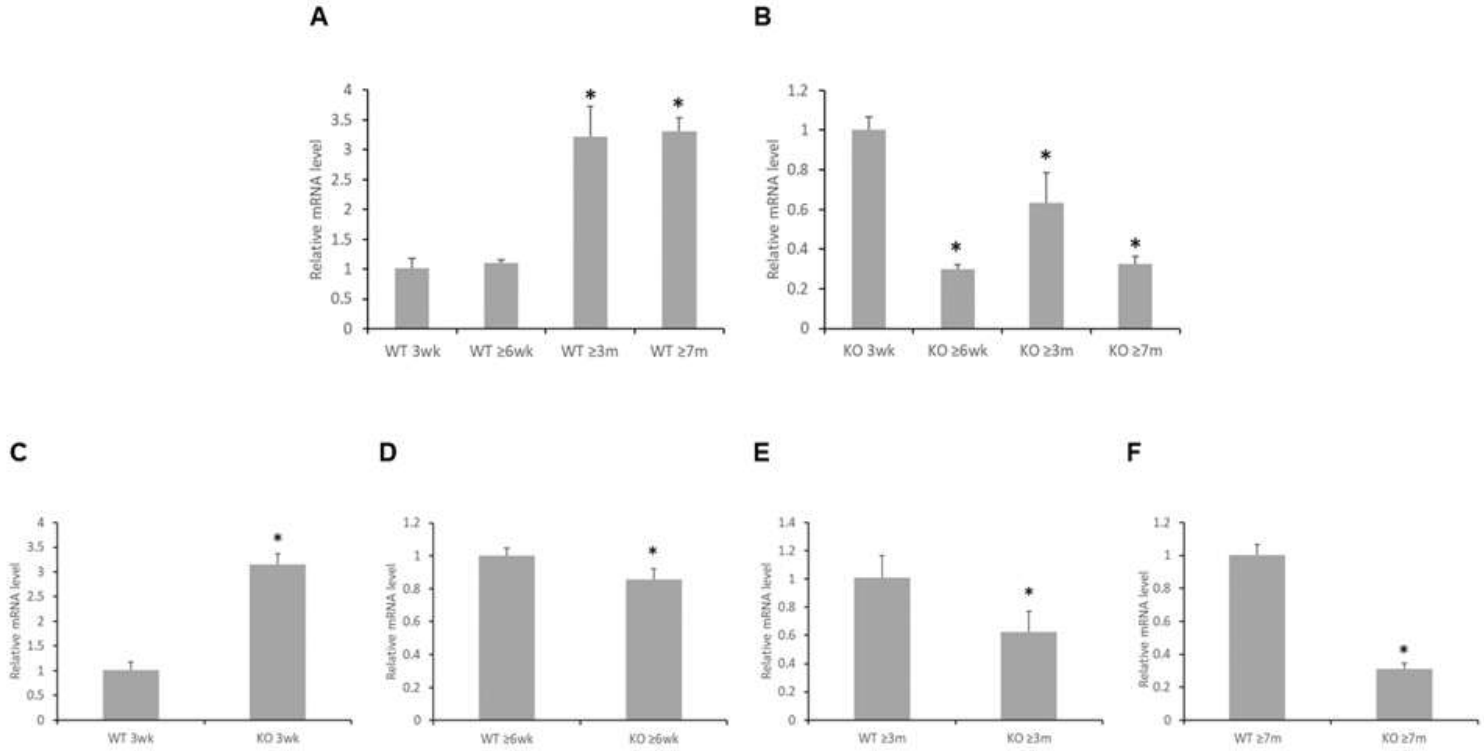

Figure 6. Relative *Kit* mRNA level on mouse ovaries. (A – B) Relative *Kit* mRNA level changes in (A) wild type and (B) *Amh* KO mice by aging. Statistical significance was evaluated versus 3-week-old wild type animals. (C – F) Relative *Kit* mRNA level changes in *Amh* KO (C) 3 wk, (D) ≥ 6 wk, (E) ≥ 3 m and (F) ≥ 7 m mice, compared with wild type mice. Data are presented as means ± standard deviation. $*P < 0.05$.

Gdnf was not changed by aging in wild type and decreased in aged *Amh* KO mice

GDNF also induces primordial-primary follicle transition. Compared with 3 wks old wild type, relative *Gdnf* mRNA level didn't change in wild type groups (Fig. 7A). In *Amh* KO mice *Gdnf* decreased in ≥ 6 wk, ≥ 3 m and ≥ 7 m compared with immature mice (Fig. 7B). Compared with the wild type groups in the same range of age, *Gdnf* increased in *Amh* KO 3 wk and ≥ 3 m and decreased in ≥ 7 m (Fig. 7C-F). *Gdnf* also decreased in old *Amh* KO mice as other earlier two genes. Thus, *Amh* doesn't inhibit primordial-primary follicle transition by inhibition of *Gdnf* as well.

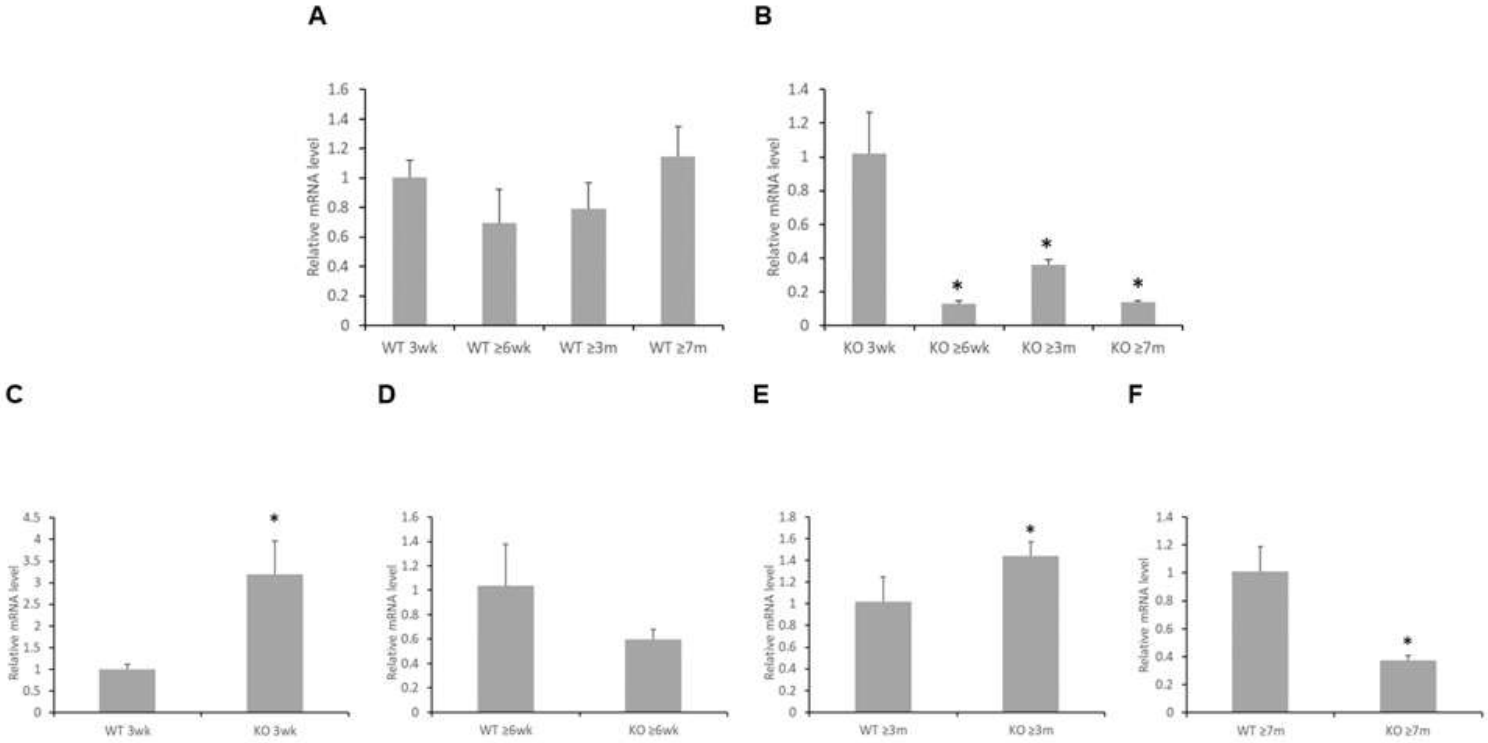

Figure 7. Relative *Gdnf* mRNA level on mouse ovaries. (A - B) Relative *Gdnf* mRNA level changes in (A) wild type and (B) *Amh* KO mice by aging. Statistical significance was evaluated versus 3-week-old wild type animals. (C - F) Relative *Gdnf* mRNA level changes in *Amh* KO (C) 3 wk, (D) ≥ 6 wk, (E) ≥ 3 m and (F) ≥ 7 m mice, compared with wild type mice. Data are presented as means ± standard deviation. $*P < 0.05$.

Gfra1 wasn't different between wild type and *Amh* KO mice

GFRA1 also involves in primordial-primary follicle transition as the receptor of GDNF. In wild type groups relative *Gfra1* mRNA level decreased in ≥ 6 wk and ≥ 3 m compared with 3 wk (Fig. 8A). In *Amh* KO mice groups *Gfra1* decreased in all of the mature age groups compared with the immature 3 wk group (Fig. 8B). Compared with the wild type groups in the same range of age, there was no significant change in *Gfra1* in any group (Fig. 8C-F). *Gfra1* didn't increase in old *Amh* KO group either like former genes, so it is considered that *Amh* doesn't inhibit primordial-primary follicle transition by downregulating Gfra1.

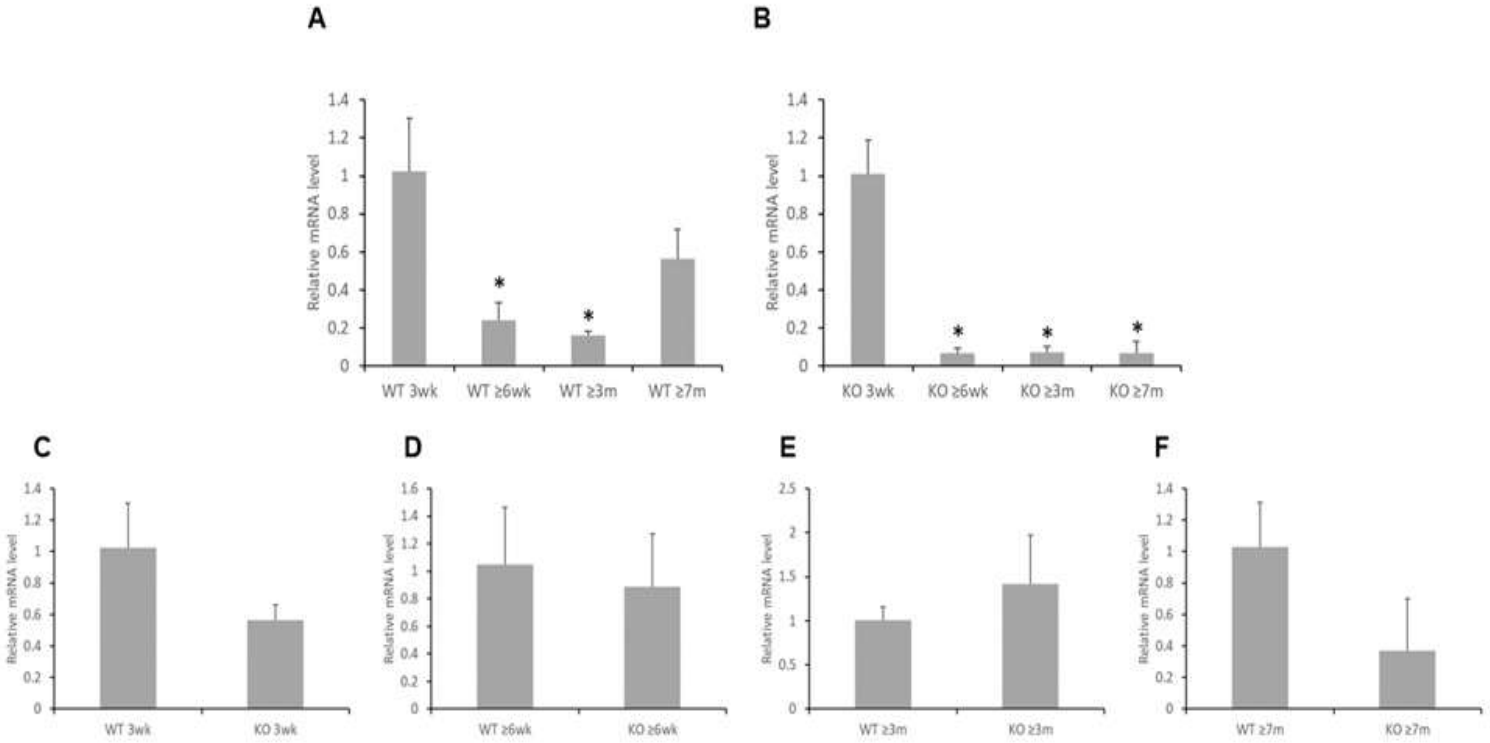

Figure 8. Relative *Gfra1* mRNA level on mouse ovaries. (A - B) Relative *Gfra1* mRNA level changes in (A) wild type and (B) *Amh* KO mice by aging. Statistical significance was evaluated versus 3-week-old wild type animals. (C - F) Relative *Gfra1* mRNA level changes in *Amh* KO (C) 3 wk, (D) ≥ 6 wk, (E) ≥ 3 m and (F) ≥ 7 m mice, compared with wild type mice. Data are presented as means ± standard deviation. $*P < 0.05$.

Bmpr1a increased by aging in wild type and decreased in aged *Amh* KO mice

Bmpr1a is a type I receptor of AMH. In wild type groups relative *Bmpr1a* mRNA level decreased in ≥ 6 wk and increased in ≥ 3 m and ≥ 7 m compared with 3 wks old wild type (Fig. 9A). In *Amh* KO groups *Bmpr1a* decreased in all ≥ 6 wk, ≥ 3 m and ≥ 7 m compared with 3 wks old *Amh* KO mice (Fig. 9B). Compared with the wild type groups in the same range of age, *Bmpr1a* increased in ≥ 6 wk and decreased in ≥ 3 m and ≥ 7 m (Fig. 9C-F). *Bmpr1a* decreased in old *Amh* KO mice compared with wild type, so AMH may amplify its own activation by enhancing its receptor, BMPR1a.

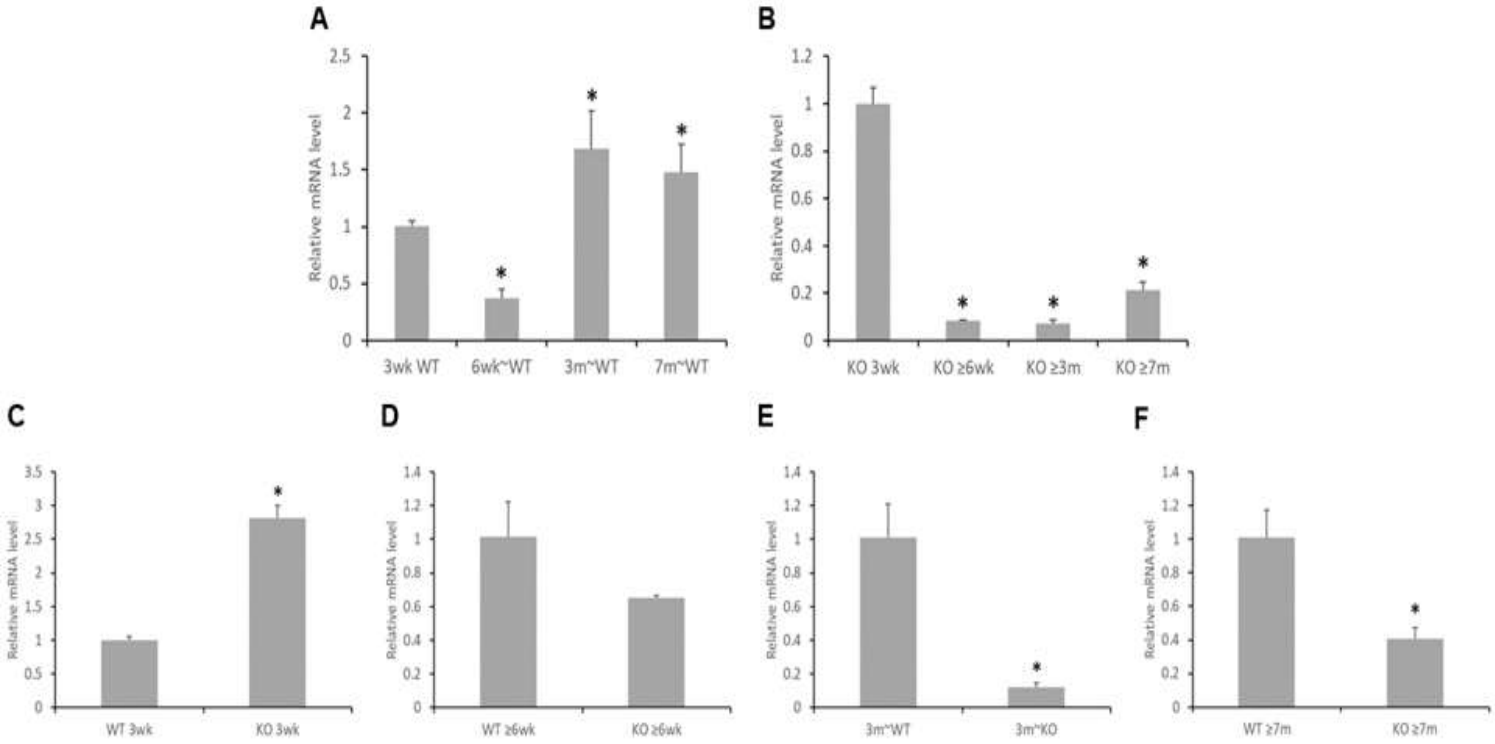

Fig 9. Relative *Bmpr1a* mRNA level on mouse ovaries. (A - B) Relative *Bmpr1a* mRNA level changes in (A) wild type and (B) *Amh* KO mice by aging. Statistical significance was evaluated versus 3-week-old wild type animals. (C - F) Relative *Bmpr1a* mRNA level changes in *Amh* KO (C) 3 wk, (D) ≥ 6 wk, (E) ≥ 3 m and (F) ≥ 7 m mice, compared with wild type mice. Data are presented as means ± standard deviation. $*P < 0.05$.

Relative p-YAP to YAP protein decreased in mature *Amh* KO mice

Compared with wild type, YAP was decreased in 3 wk, ≥ 6 wk, ≥ 7 m *Amh* KO mice and increased in the ≥ 6 wk KO group (Fig. 10A,C). TAZ was increased in ≥ 6 wk, and decreased in ≥ 7 m group (Fig. 10A,D). phosphorylated YAP (p-YAP) was increased in 3 wk, ≥ 6 wk, ≥ 3 m and ≥ 7 m groups (Fig. 10B,E). Relative p-YAP to YAP level was calculated for inactivation of YAP/TAZ, inhibiting nuclear translocation of YAP/YAZ to translate proliferative factors and follicle development (Fig. 10F). p-YAP/YAP was in creased in 3 wk, but decreased ≥ 6 wk, ≥ 3 m and ≥ 7 m.

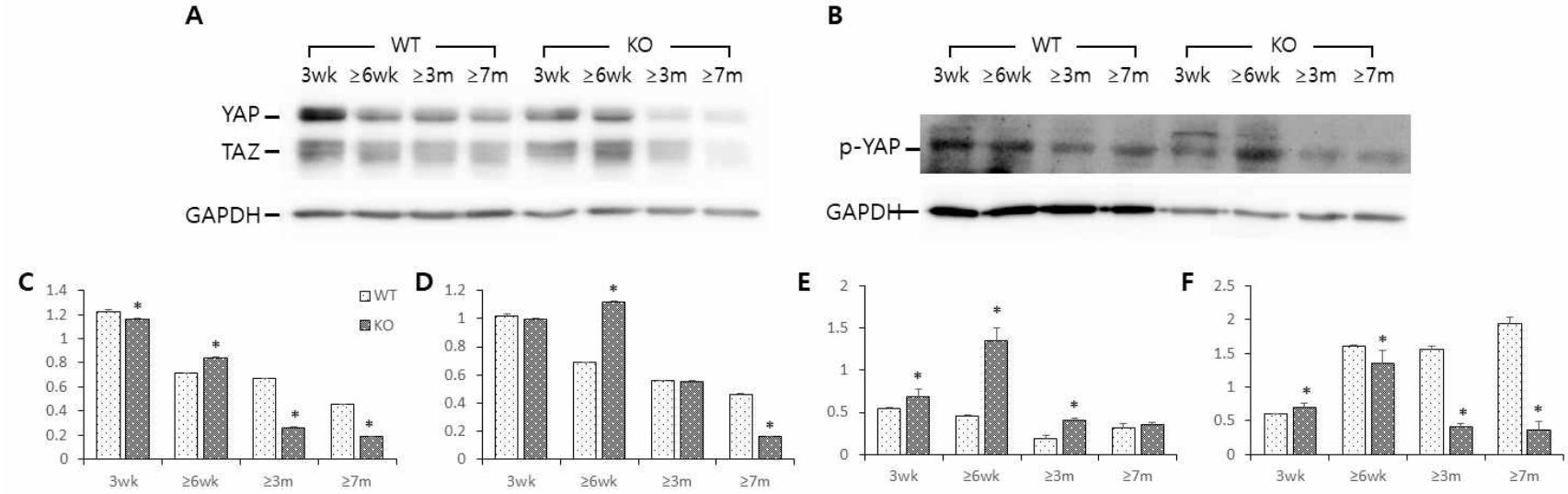

Fig 10. Protein expression profiles of YAP and TAZ on mouse ovaries. Western blot analysis of ovaries of 3 wk, ≥ 6 wk, ≥ 3 m and ≥ 7 m old wild type and *Amh* KO mice for (A, C) YAP, (A, D) TAZ and (B, E) phosphorylated YAP (p-YAP). The target protein levels were normalized to GAPDH. (F) Relative p-YAP to YAP (p-YAP/YAP).

Localization of YAP/TAZ and p-YAP did not change in *Amh* KO mice

YAP/TAZ predominantly located in cytoplasm of oocytes and GCs and nuclei of thcal cells in all non-atretic follicles (Fig. 11). In atretic follicles, it was observed in nuclei of GCs and thecal cells, but not in atretic cells. The localization pattern didn' t change regardless of age and was same in *Amh* KO mice as well. p-YAP was located in nuclei of oocytes, GCs and thecal cells and cytoplasm of oocytes in all follicles (Fig. 12). Likewise, It wasn' t different in *Amh* KO mice.

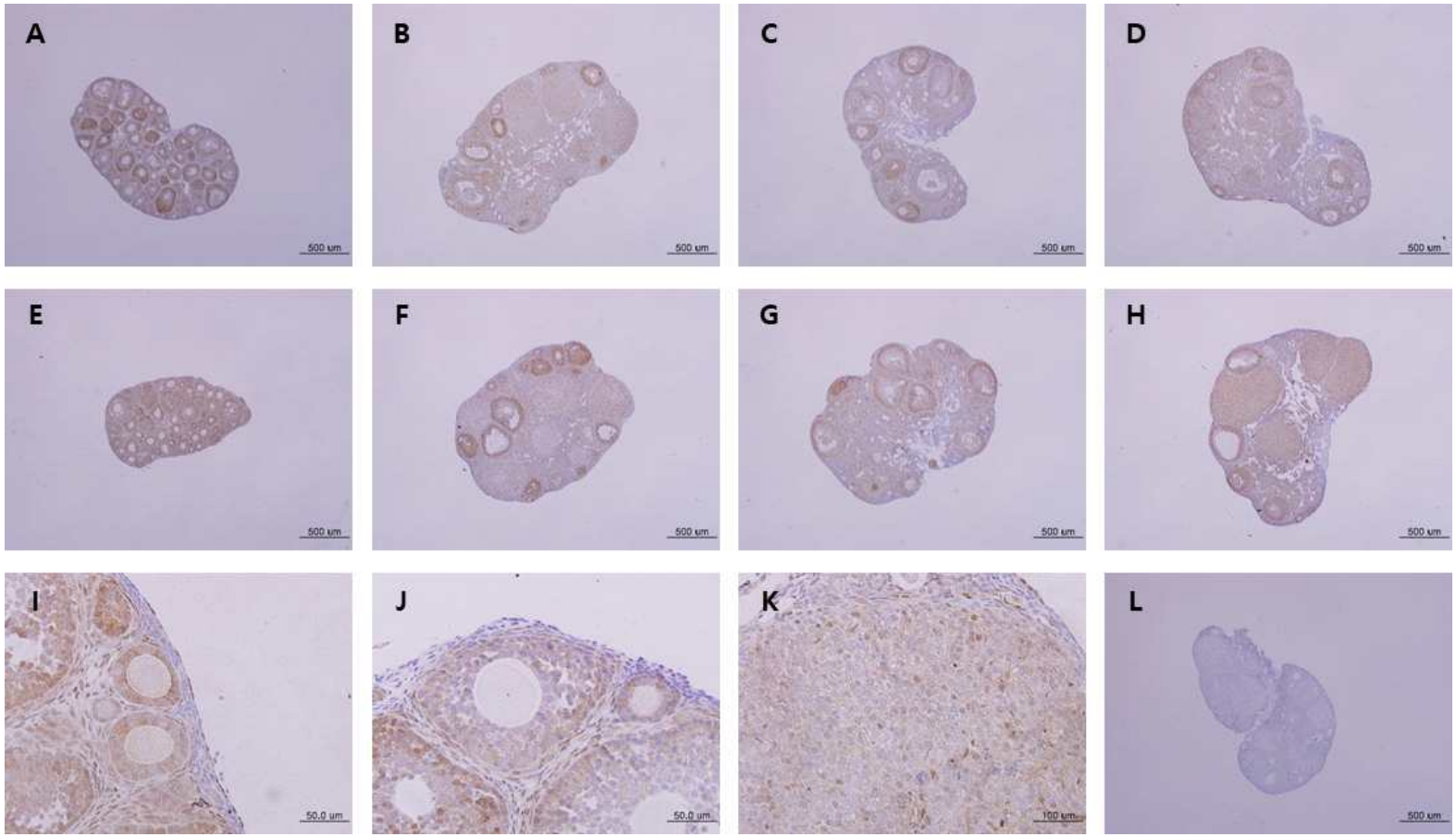

Fig 11. Immunohistochemistry of YAP/TAZ in ovaries. (A – D) Wild type. (E – H) *Amh* KO. (I – K) YAP/TAZ localization in follicles and CL. (L) Negative control.

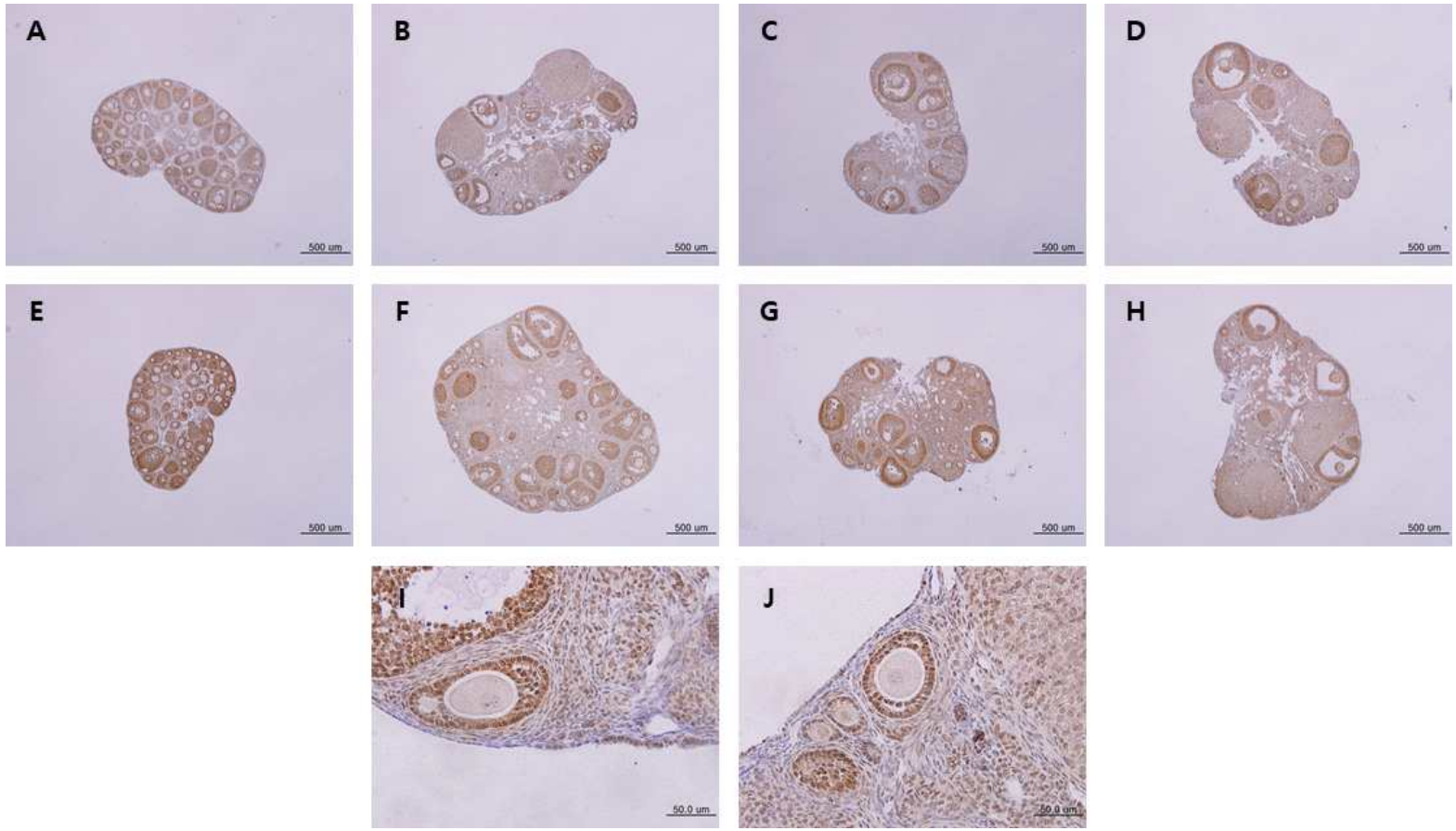

Fig 12. Immunohistochemistry of p-YAP in ovaries. (A - D) Wild type. (E - H) *Amh* KO. (I - J) YAP/TAZ localization in follicles and CL.

DISCUSSION

AMH is considered to be related to ovarian reserve and ovarian aging, inhibiting primordial-primary follicle transition (Zec *et al.*, 2011). Serum AMH levels decrease with age and drop to undetectable levels in menopausal women (de Vet *et al.*, 2002). Therefore, serum AMH levels are often measured as an ovarian reserve indicator in clinic. Recently the researches for ovarian reservation is focused on basic and medical sciences, but the age-dependent role of AMH is not much uncovered.

We investigated if deletion of AMH can affect fertility with age even if female AMH KO mice is known to have fertility, as AMH serum level is important in human for that. In *Amh* KO mice, the fertility was dramatically decreased from 7 m compared to wild type but not until 6 m. These results mean that AMH may have important function in folliculogenesis.

The number of primordial and primary follicles in *Amh* KO mice was smaller than those of wild type mice over 7 m. However, the number of primordial follicle was more that those of the wild type until 6 months. However, previously, it was reported that AMH block the transition of primordial to primary follicle. It may be caused by the age of the AMH KO.

Kit ligand (*Kitl*), its receptor, c-kit (*Kit*), *Gdnf* and GDNF receptor α1 (*Gfra1*) are known as inducers for primordial-primary follicle transition on the contrary to AMH

(Dole G *et al.*, 2008). With age, their mRNA level changes were demonstrated to know if AMH have negative action on primordial-primary follicle transition by inhibiting them.

Müllerian duct studies revealed that AMH signals through the same pathway as the BMP families that a serine-threonine kinase receptor complex consisting of type I receptors which are also known as activin receptor-like protein kinases (ALKs) and type II receptors (Jamin *et al.*, 2002). ALK2 and ALK3 are expressed in the granulosa cells of small growing follicles. ALK6 is expressed in the mouse ovary, but mostly in antral follicles (Erickson and Shimasaki, 2003; Yi *et al.*, 2001). Among them we revealed mRNA level of ALK3 that is also called as BMPR1A.

In Hippo pathway, when YAP and TAZ are activated they translocate into nuclei and induce transcription of genes that are related to cell proliferation, differentiation, migration (Meng Z *et al.*, 2016). YAP/TAZ is inactivated by phosphorylation. It was suggested that primordial follicle activation is related to decrease in ratio of phosphorylated YAP1 (p-YAP)/YAP1 (Xiang C *et al.*, 2015). Ovarian fragmentation decreased p-YAP and increased nuclear localization of YAP, leading to follicle growth (Kawamura *et al.*, 2013).

In summary, the fertility of the *Amh* KO was decreased 7 months after birth. The number of primordial follicles was well not decreased compared with wild type. *Kitl*, *Kit*, *Gdnf*, *Graa1*, *Bmpr1a* mRNAs and *Kit* mRNA gradually increased by aging after maturation. However, there expression profiles in *Amh* knockout mice were differnet from wild type. The

expression levels of *Bmpr1a* mRNA, type I receptor of AMH, were decreased in ≥ 3 m and ≥7 m *Amh* knockout groups compared to wild type. On the other hand YAP activity was significantly decreased from 6 wks to older age. Based on these results, it issuggested that AMH may control the primordial-to-primary follicle transition and AMH and YAP signaling may involved in the control the ovarian reservation. *Kitl*, *Kit*, *Gdnf*, *Gfra1* and *Bmpr1a* mRNA gradually increased by aging after maturation. However, the expression profiles in *Amh* KO mice were different from wild type. The expression levels of *Bmpr1a* mRNA, type I receptor of AMH, were decreased in ≥ 3 m and ≥7 m *Amh* KO groups compared to wild type. On the other hand, YAP activity was significantly decreased from 6 wks to older age. Based on these results, it is suggested that AMH may control the primordial-primary follicle transition and AMH and YAP signaling may involve in control of ovarian reservation.

REFERENCE

Baarends WM, Uilenbroek JT, Kramer P, Hoogerbrugge JW, van Leeuwen EC, Themmen AP, Grootegoed JA. 1995. Anti-Müllerian hormone and anti-Müllerian hormone type II receptor messenger ribonucleic acid expression in rat ovaries during postnatal development, the estrous cycle, and gonadotropin-induced follicle growth. Endocrinology 136:4951-4962.

Behringer RR, Finegold MJ, Cate RL. 1994. Mü llerian-inhibiting substance function during mammalian sexual development. Cell 79:415-425.

de Vet A, Laven JSE, de Jong FH, Themmen APN, Fauser BCJM. 2002. AntiMüllerian hormone serum levels: a putative marker for ovarian aging. Fertil Steril 77:357-362.

Dole G, Nilsson EE, Skinner MK. 2008. Glial-derived neurotrophic factor promotes ovarian primordial follicle development and cell-cell interactions during folliculogenesis. Reproduction 135:671-682.

Durlinger ALL, Kramer P, Karels B, Jong FHD, Uilenbroek JTJ, Grootegoed JA, Themmen APN. 1999. Control of primordial follicle recruitment by Anti-Müllerian Hormone in the mouse ovary. Endocrinology 140:5789-5796.

Erickson GF, Shimasaki S. 2003. The spatiotemporal expression pattern of the bone morphogenetic protein family in rat ovary cell types during the estrous cycle.

Reprod Biol Endocrionol. 1:9.

Hirobe S, He WW, Lee MM, Donahoe PK. 1992. Müllerian inhibiting substance messenger ribonucleic acid expression in granulosa and Sertoli cells coincides with their mitotic activity. Endocrinology 131:854-862.

Jamin SP, Arango NA, Mishina Y, Hanks MC, Behringer RR. 2002. Requirement of *Bmpr1a* for Müllerian duct regression during male sexual development. Nat Genet. 32:408-410.

Kawamura K, Cheng Y, Suzuki N, Denguchi M, Sato Y, Takae S, Ho CH, Kawamura N, Tamura M, Hashimoto S, Sugishita Y, Morimoto Y, Hosoi Y, Yoshioka N, Ishizuka B, Hsueh AJ. 2013. Hippo signaling disruption and Akt stimulation of ovarian follicles for infertility treatment. Proc Natl Acad Sci USA. 110:17474-17479.

Meng Z, Moroishi T, and Guan KL. 2016. Mechanisms of Hippo pathway regulation. Gene Dev 30:1-17.

Parrott JA, Skinner MK. 1999. Kit-ligand/stem cell factor induces primordial follicle development and initiates folliculogenesis. Endocrinology 140:4262-4271.

Visser JA, Themmen APN. 2004. Anti-Müllerian hormone and folliculogenesis. Mol Cell Endocrinol 234:81-86.

Xiang C, Li J, Hu L, Huang J, Luo T, Zhong Z, Zheng Y, Zheng L. 2015. Hippo signaling pathway reveals a spatio-temporal correlation with the size of primordial follicle pool in mice. Cell Physiol Biochem 35:957-968.

Yi SE, LaPolt PS, Yoon BS, Chen JY, Lu JK, Lyons KM. 2001. The type I BMP receptor BmprIB is essential for female reproductive function. Proc Natl Acad Sci USA.

98:7994-7999.

Zec I, Tislaric-Medenjak D, Megla ZB, Kucak I. 2011. Anti-Müllerian hormone: a unique biochemical marker of gonadal development and fertility in humans. Biochem Med 21:219-230.

논 문 개 요

암컷에서 anti-Müllerian hormone (AMH)은 난소의 성장난포의 과립세포에서 생산 및 방출되어 원시난포가 일차난포로 발생되는 것을 억제하고, 전동난포가 동난포로 발생되게 하는 FSH에 대한 민감도를 감소시킨다. 따라서 AMH는 난소 노화와 관련이 있다고 여겨진다. 실제로 혈중 AMH 농도는 나이가 듦에 따라 감소한다. 7~11 개월령의 나이 든 암컷 *Amh* 적중 생쥐는 같은 나이대의 야생형 동물에 비해 낮은 출산율의 경향성을 나타냈다. 이 논문에서는 이러한 표현형에 근거하여 *Amh* 적중 생쥐의 난소 샘플에서 원시난포-일차난포 전환에 관여한다고 알려져있는 유전자들인 *Kitl*, Kit, Gdnf, Gfra1을 표적하여 qPCR을 진행해서 노화에 따라 이 유전자들의 mRNA 수치 변화의 경향성과 AMH가 이 유전자들을 억제하여 난포동원을 조절하는지를 알고자 하였다. 3개월령 이상의 *Amh* 적중 생쥐에서 *Kitl*, *Kit*, *Gdnf*, *Bmpr1a* mRNA는 야생형보다 감소하였고, *Gfra1*의 경우에는 7개월령 이후에만 감소하였다. AMH의 type I 수용체인 *Bmpr1a* mRNA의 발현은 *Amh* 적중 생쥐의 경우 3개월부터 야생형에 비하여 그 발현양이 유의하게 감소하였다. 이러한 결과를 통하여 AMH가 그 수용체를 기반으로 원시난포-일차난포 전이를 조절하고 YAP 신호와 관련되어 난소 예비력에 관여할 것으로 사려된다.

감사의 글

끝나지 않을 것만 같았던 2년 동안의 석사 과정이 무사히 막을 내림에 감사합니다.

먼저, 과학자로서 확고한 철학을 가지고 연구에 임하는 모습이 존경스러운 전용필 지도 교수님, 저를 학문의 길로 인도해주심에, 그리고 새로운 기회를 주심에 감사드립니다. 논문 심사를 해주신 미래와 희망 산부인과 박종혁 박사님, 글로벌의학과 전민영 교수님과 아낌없는 코멘트를 주신 서울여자대학교 김해권 교수님, 상명대학교 이성호 교수님께 감사드립니다. 제가 생명과학이란 학문을 흥미를 느끼게 해주신 본교 강혜순 교수님, 윤진호 교수님, 김상태 교수님, 강창수 교수님, 최상철 교수님께 감사드립니다.

거의 매일 하루 종일 같이 생활했는데도 갈등 없이 서로 독려하며 힘이 되어준 가족 같은 세 명의 동기, 희선 언니, 우리 언니, 민영이 덕분에 즐거운 랩 생활이 될 수 있었습니다. 또, 언제나 열린 마음으로 실험하는 데 많은 도움을 준 학문에 열정적인 순영 언니, 누구보다 부지런한 연정 언니에게 감사합니다. 나를 이어 *Amh* KO mice를 이어받아 관리하는 주은이도 고맙고, 입학 축하한다. Cheon’ s lab 식구 모두 좋은 결실을 맺고 밝은 미래를 기원합니다.

미래와 희망 황희경 선생님, 강안에스 선생님, 유자현 선생님, 조환희 선생님, 정이와 선생님, 김소현 선생님 그리고 다시 한 번 박종혁 실장님께 학업과 일을 병행하느라 배려하고 양해해 주신 부분들, 부족한 저를 이끌어 가주심에 감사드리고, 죄송스런 마음입니다. 이제 맑은 정신으로 일에 더 집중하고 나아가는 모습 보여드리겠습니다.

항상 멀리서 저를 위해 기도해주신 할머니들, 늘 감사하고 건강하시길 바라요. 군대에서 나라 지키느라 고생하는 주승이도 고맙고, 너에게도 앞으로 1년이란 세월이 평탄하고 빠르게 지나가고, 건강하게 돌아오길 바란다. 매일 딸한테서 따뜻한 전화 한 통화만을 기다리며, 딸 문제라면 멀리서도 한

달음에 달려오시는 내 편 우리 엄마, 아빠, 바쁘다는 핑계로 오랜 기간 집에 들리지 못해 미안하고, 고마워요. 이제는 제가 그 은혜에 보답하는 딸이 될게요. 루나는 항상 건강하게 있어주는 것만으로 고맙고 보고 싶다. 곧 보러갈게. 멀리서도 항상 우울하고 지칠 때 나 대신 나를 사랑해주고 긍정의 말들로 내가 버틸 수 있게 도와준 Marin도 항상 고맙고 그립고 사랑해.

그 외, 지면에 다 싣지 못한 모든 분들께도 감사드립니다.